ADVANCES IN ATMOSPHERIC SCIENCES, 2024

• **News & Views** •

Extreme Antarctic Cold of Late Winter 2023

Anastasia J. TOMANEK[1], David E. MIKOLAJCZYK[*1], Matthew A. LAZZARA[1,2], Stefano DI BATTISTA[3], Minghu DING[4], Mariana FONTOLAN LITELL[5,6], David H. BROMWICH[5], Taylor P. NORTON[1], Linda M. KELLER[1], and Lee J. WELHOUSE[1]

[1]*Antarctic Meteorological Research and Data Center*, *Space Science and Engineering Center*, *University of Wisconsin-Madison*, *Madison*, *Wisconsin* 53706, *USA*

[2]*Department of Physical Sciences*, *School of Engineering*, *Science*, *and Mathematics*, *Madison Area Technical College*, *Madison*, *Wisconsin* 53704, *USA*

[3]*Meteogiornale*, *via Paolo Diacono*, *9*, *Milano* 20133, *Italy*

[4]*State Key Laboratory of Severe Weather*, *Chinese Academy of Meteorological Sciences*, *Beijing* 100081, *China*

[5]*Byrd Polar and Climate Research Center*, *The Ohio State University*, *Columbus*, *Ohio* 43210, *USA*

[6]*Department of Geography*, *The Ohio State University*, *Columbus*, *Ohio* 43210, *USA*

(Received 21 April 2024; revised 11 May 2024; accepted 16 May 2024)

ABSTRACT

Extreme cold temperatures were observed in July and August 2023, coinciding with the WINFLY (winter fly-in) period of mid to late August into September 2023, meaning aircraft operations into McMurdo Station and Phoenix Airfield were adversely impacted. Specifically, with temperatures below −50°C, safe flight operation was not possible because of the risk of failing hydraulics and fuel turning to gel onboard the aircraft. The cold temperatures were measured across a broad area of the Antarctic, from East Antarctica toward the Ross Ice Shelf, and stretching across West Antarctica to the Antarctic Peninsula. A review of automatic weather station measurements and staffed station observations revealed a series of sites recording new record low temperatures. Four separate cold phases were identified, each a few days in duration and occurring from mid-July to the end of August 2023. A brief analysis of 500-hPa geopotential height anomalies shows how the mid-tropospheric atmospheric environment evolves in relation to these extreme cold temperatures. The monthly 500-hPa geopotential height anomalies show strong negative anomalies in August. Examination of composite geopotential height anomalies during each of the four cold phases suggests various factors leading to cold temperatures, including both southerly off-content flow and calm atmospheric conditions. Understanding the atmospheric environment that leads to such extreme cold temperatures can improve prediction of such events and benefit Antarctic operations and the study of Antarctic meteorology and climatology.

Key words: Antarctica, extreme cold, temperature, automatic weather station networks

Citation: Tomanek, A. J., and Coauthors, 2024: Extreme Antarctic cold of late winter 2023. *Adv. Atmos. Sci.*, https://doi.org/10.1007/s00376-024-4139-1.

Article Highlights:

- Record cold temperatures observed across a portion of the Antarctic in August and September 2023.
- Aviation operations impacted during this period because of the extreme cold.
- The orientation of the 500-hPa pattern hints at the large-scale pattern during the event.

1. Introduction

In July and August 2023, an outbreak of record cold temperatures was observed across a segment of the Antarctic, especially in East Antarctica toward the Ross Ice Shelf (RIS). Several locations experienced cold temperatures during this period, breaking prior record lows (Table 1). Antarctica experiences extreme temperatures, both warm and cold, including the coldest observed on the planet (Skansi et al., 2017; Turner et al., 2021; Keller et al., 2022). Various event analyses have

* Corresponding author: David E. MIKOLAJCZYK
Email: david.mikolajczyk@ssec.wisc.edu

yielded different definitions of what is considered an extreme event, but determining a suitable definition is dependent on the meteorological parameters exceeding the mean (Turner et al., 2021).

Extreme cold temperatures most often occur in July and August, though they can be observed in June and September during the extended winter season (Turner et al., 2009). Favorable conditions for anomalous low temperatures include isolation from mild midlatitude air masses for extended periods and extensive sea-ice cover in the vicinity of the station to limit heat and moisture fluxes from the ocean (Turner et al., 2021). Conditions, in this case, led to an interference in the US Antarctic Program's winter fly-in (WINFLY) operations to Phoenix Airfield. WINFLY is the first arrival of cargo, supplies, and support staff to McMurdo Station for its operational field season. Significantly colder than normal temperatures can interrupt or even halt the operation. Aircraft are not able to operate when temperatures are below −50°C at the ground, with additional limiting thresholds of −55°C in-flight, −54°C for the hydraulics, and −58°C for the fuel (Lazzara et al., 2012).

2. Data

Observations from a sample of both automatic weather stations (AWSs) and staffed stations (Fig. 1) were examined for this weather event. AWS observations from the UW-Madison Antarctic Meteorological Research and Data Center (AMRDC) AWS program (Lazzara et al., 2012) and State Key Laboratory of Severe Weather AWS program (Ding et al., 2022) were primarily used for event analysis. Data from the UW-Madison AWS program are quality controlled [as outlined in Lazzara et al. (2012)], as were AWS observations along PANDA networks [detailed specifications can be found in Ding et al. (2022)]. Hourly temperature observations provided by the State Key Laboratory of Severe Weather AWS program detailed observations at Great Wall Station, Zhongshan Station, and Taishan AWS (Figs. 1 and 2). Ten-minute quality-controlled observations were additionally provided by the UW-Madison AMRDC AWS program for Windless Bight, Margaret, and Byrd AWS (Figs. 1 and 2). Reanalysis data from ERA5 (Hersbach et al., 2020) are used to illustrate the cold air pool at 500 hPa via composite analysis.

In terms of data reliability, the quality of AWS temperature data is generally lower than that of data recorded at staffed stations. In winter, the influence of solar radiation combined with calm winds on the air temperature (Genthon et al., 2011) is absent, but the sensor may have other problems. The height of the sensor above the surface gradually decreases as snow accumulates on the ground, which normally results in slightly lower temperatures until the AWS is lifted during routine maintenance (Turner et al., 2004). However, this maintenance cannot be guaranteed every year (Lazzara et al., 2012). This may contribute to cold records slightly lower than what occurred, but the same could also be true for past records. Obviously, a sensor in these conditions will also give a slightly lower monthly average. But in the monthly average, the problem of missing

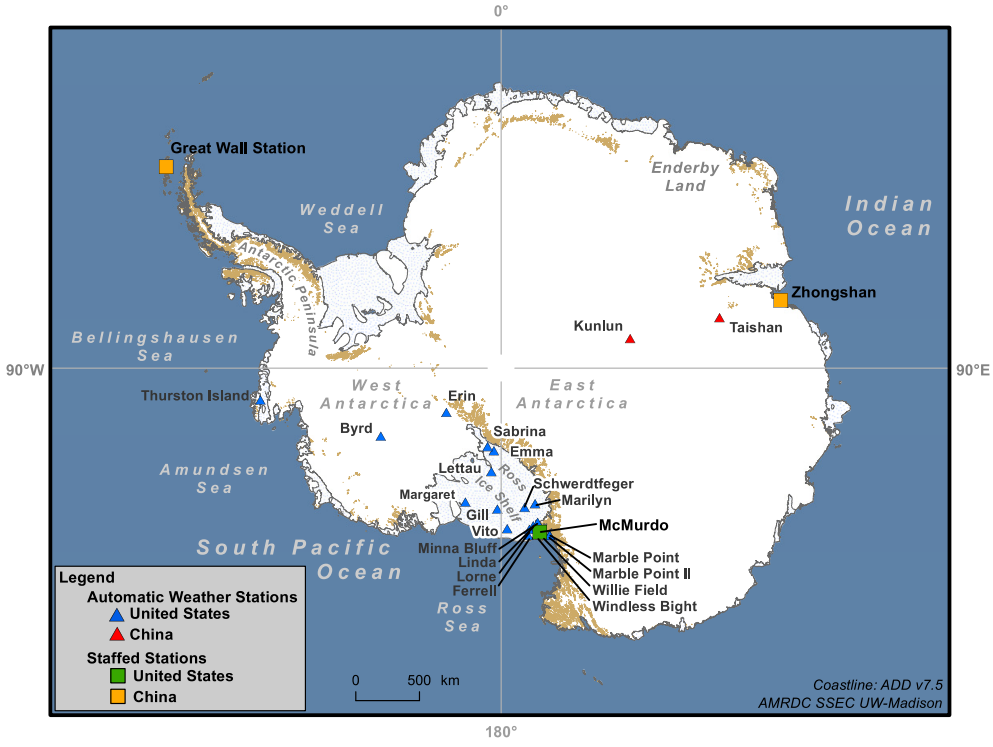

Fig. 1. Map of the Antarctic continent with AWSs and staffed stations referenced for the extreme cold event. Colors and shapes indicate the type of station and country it is managed by.

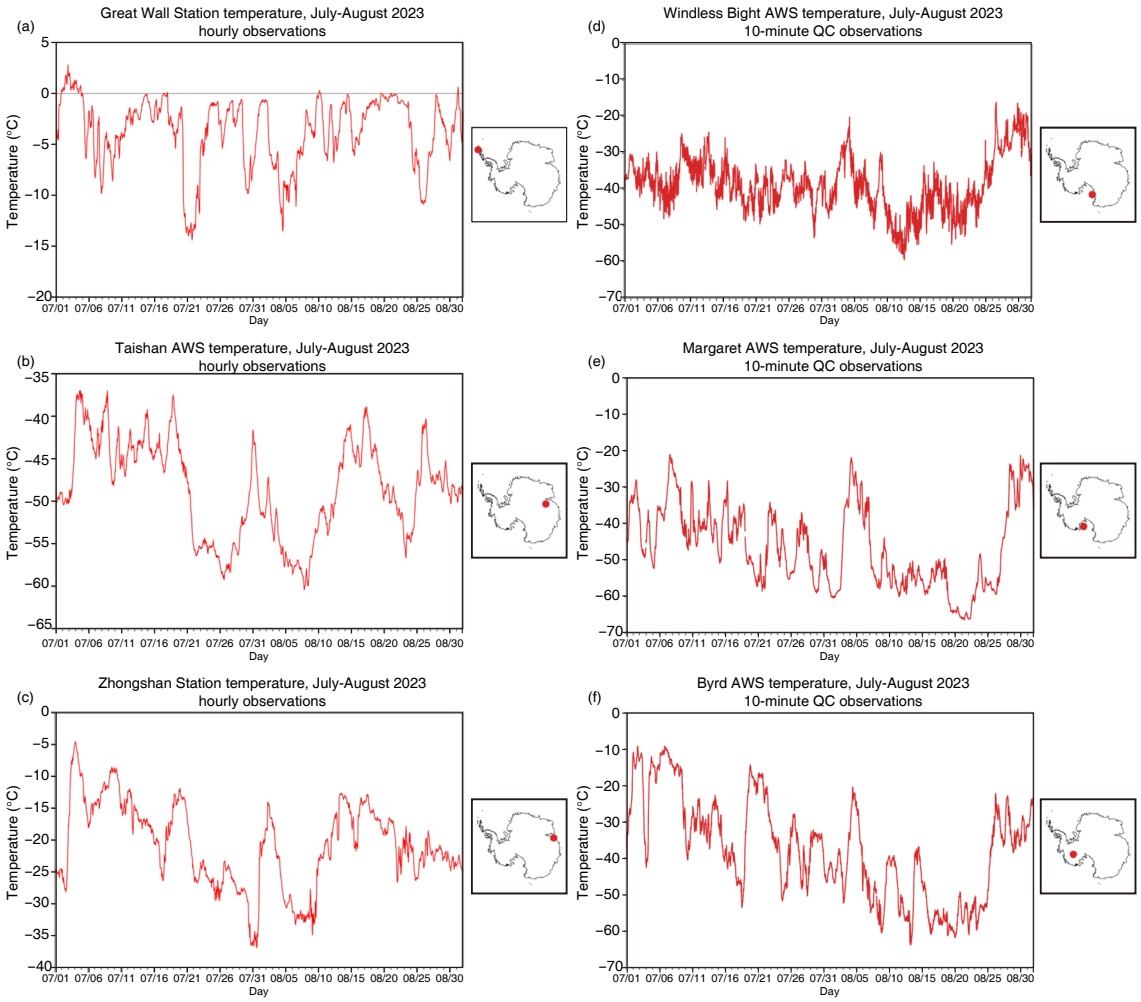

Fig. 2. Hourly temperature observations for July and August of 2023 at (a) Great Wall Station, (b) Taishan AWS, and (c) Zhongshan Station provided by Minghu DING. 10-minute quality-controlled temperature observations for July and August of 2023 at (d) Windless Bight AWS, (e) Margaret AWS and (f) Byrd AWS provided by the AMRDC.

data is more important. For example, Vito AWS data are missing between 1 and 2 August. If the missing data are for very cold or very hot days, the monthly average can be altered.

3. Records

After reviewing the UW-Madison AWS observational data, Table 1 outlines the record temperatures recorded during this period.

3.1. *Absolute temperatures*

Some Antarctic regions experienced extreme cold in August 2023—namely, West Antarctica (WA) or Marie Byrd Land, RIS, and Ross Island Vicinity (RIV). These three regions cover approximately 2.1 million km^2 of the Antarctic continent. The cold began in mid-July and had four main phases: 21–23 July, 31 July–1 August, 10–13 August, and 19–24 August. In the AMRDC network, 13 AWSs broke record lows (Table 1), while some AWSs broke a record of at least 30 years or across their period of record.

The new records, in some cases repeated days later, exhibited how the event was incisive and persistent. The value reached at Margaret (−66.4°C) is noteworthy: it is the second-coldest minimum ever recorded in these Antarctic regions after Emilia (−66.9°C on 14 April 2013). As a suggestive corollary, the Terra Nova Expedition, which surveyed very different conditions compared to the AWS, measured −77.5°F (−60.8°C) on 6 July 1911 at Windless Bight (Cherry-Garrard, 1922).

Cold values within 1°C of the record minimum (Table 1b) were also observed. Those at Byrd, Ferrell, and Lettau are

Table 1. (a) 2023 record low temperatures (°C) listed by station, region, and date of the last record low temperature. (b) Stations that came within 1°C of the previously recorded low temperature. (c) Monthly average temperature (°C) and deviation from the monthly average for July–August 2023 by station and region.

(a) Record lows

Name	Elevation (m)	Region	Start	Previous minimum (date, °C)	Minimum 2023 (UTC, °C)
Emma	76	RIS	2014	28 July 2016, −56.9°C	11 August (1220, −57.4°C) 12 August (1240, −59.6°C) 22 August (2130, −60.6°C) 23 August (0950, −60.9°C)
Erin	988	WA	1994	16 July 2010, −53.2°C	12 August (1010, −53.9°C)
Linda	41	RIV	1991	18 July 2010, −54.9°C	10 August (2340, −55.1°C) 11 August (2350, −56.9°C) 12 August (0230, −57.7°C)
Lorne	44	RIV	2007	17 July 2010, −54.9°C	10 August (2350, −55.4°C) 11 August (0810, −58.1°C)
Marble Point	108	RIV	1980	17 July 2010, −45.6°C	12 August (1400, −46.2°C)
Marble Point II	111	RIV	2011	30 July 2016, −39.0°C	19 July (2330, −40.5°C) 10 August (2350, −42.1°C) 11 August (0950, −43.4°C) 12 August (2100, −45.6°C)
Margaret	67	RIS	2008	18 July 2017, −64.7°C	20 August (2320, −66.0°C) 21 August (0930, −66.4°C)
Marilyn	62	RIS	1984	2 September 2009, −58.5°C	22 August (1210, −58.8°C)
Minna Bluff	895	RIV	1991	24 August 1993, −48.1°C	13 August (1000, −50.5°C)
Sabrina	87	RIS	2009	2 September 2009, −57.8°C	12 August (0900, −59.0°C) 23 August (0300, −60.0°C)
Vito	50	RIS	2004	22 August 2008, −60.6°C	13 August (1820, −61.2°C) 21 August (1030, −63.6°C)
Willie Field	9	RIV	1992	7 August 2001, −56.9°C	11 August (2250, −57.9°C) 12 August (1350, −59.9°C)
Windless Bight	40	RIV	1998	9 August 2001, −58.9°C	12 August (1510, −59.5°C)

(b) Within 1°C of record

Name	Elevation (m)	Region	Start	Current minimum (Date, °C)	Minimum 2023 (UTC, °C)
Byrd	1539	WA	1980	18 July 1985, −64.4°C	13 August (0710, −63.9°C)
Ferrell	43	RIV	1980	3 August 1990, −58.3°C	12 August (1430, −58.3°C)
Lettau	38	RIS	1986	21 August 2008, −63.1°C	12 August (1740, −62.3°C) 23 August (0700, −62.2°C)
Thurston Island	225	WA	2011	5 September 2013, −39.0°C	13 August (1310, −38.7°C)

(c) Monthly averages

Name	Elevation (m)	Region	Start	July–August average 2023 (°C)	Deviation from average (°C)
Elaine	59	RIS	1986	−38.9°C	−6.2°C
Ferrell	43	RIV	1980	−40.4°C	−6.1°C
Gill	53	RIS	1985	−46.2°C	−5.8°C
Lettau	38	RIS	1986	−46.8°C	−8.2°C
Linda	41	RIV	1991	−39.9°C	−7.5°C
Marble Point	108	RIV	1980	−31.6°C	−6.2°C
Marilyn	62	RIS	1984	−39.9°C	−7.1°C
Minna Bluff	895	RIV	1991	−32.4°C	−3.3°C
Schwerdtfeger	54	RIV	1985	−44.2°C	−6.7°C

important to note because of their long period of record. Eleven stations reached a −60°C threshold despite the conditions not occurring frequently in these regions. Elaine (−60.6°C on 12 August), Emilia (−60.1°C on 13 August), Gill (−62.6°C on 21 August), and Schwerdtfeger (−61.3°C on 21 August) were also identified in addition to those reported in Table 1a and 1b.

3.2. *Monthly averages*

Comparisons with long-term monthly averages (Table 1c) show that August 2023 was very cold at Byrd in WA. With an average of −45.5°C, it was the coldest month on record (the previous was −44.7°C in September 1986). In RIS and RIV, however, the very cold period spanned July and August. Data from McMurdo, which opened in 1956 in RIV, revealed the average temperature for the months of July and August 2023 was −31.4°C. This average is the second coldest for the period 1956–2023, after July and August 1978 (−31.5°C), i.e., in a time before the installation of the AWS. From nine selected

AWSs of RIS and RIV, the deviation of July and August averages from multi-year averages was very large, with the exception of Minna Bluff where the average of July and August 2008 reached −32.3°C, very close to the 2023 value. The multi-year averages (Table 1c) were derived using data from the Reference Antarctic Data for Environmental Research (READER; Turner et al., 2004). In some cases, the recalculated August average is different from READER by ±0.1°C.

4. Atmospheric environment

An examination of the atmospheric environment that led to these cold temperatures can be seen in the ERA5 500-hPa geopotential height anomalies during this study period (Fig. 3). The July composite geopotential height anomalies are relatively featureless over the Antarctic continent and surrounding Southern Ocean, except for a strong positive anomaly in the Ross Sea (Fig. 3a). For August, a few regions of anomalously low geopotential heights were prevalent, with strong negative anomalies over the Bellingshausen Sea near the peninsula and over the Wilkes Land region (Fig. 3b). The strong positive height

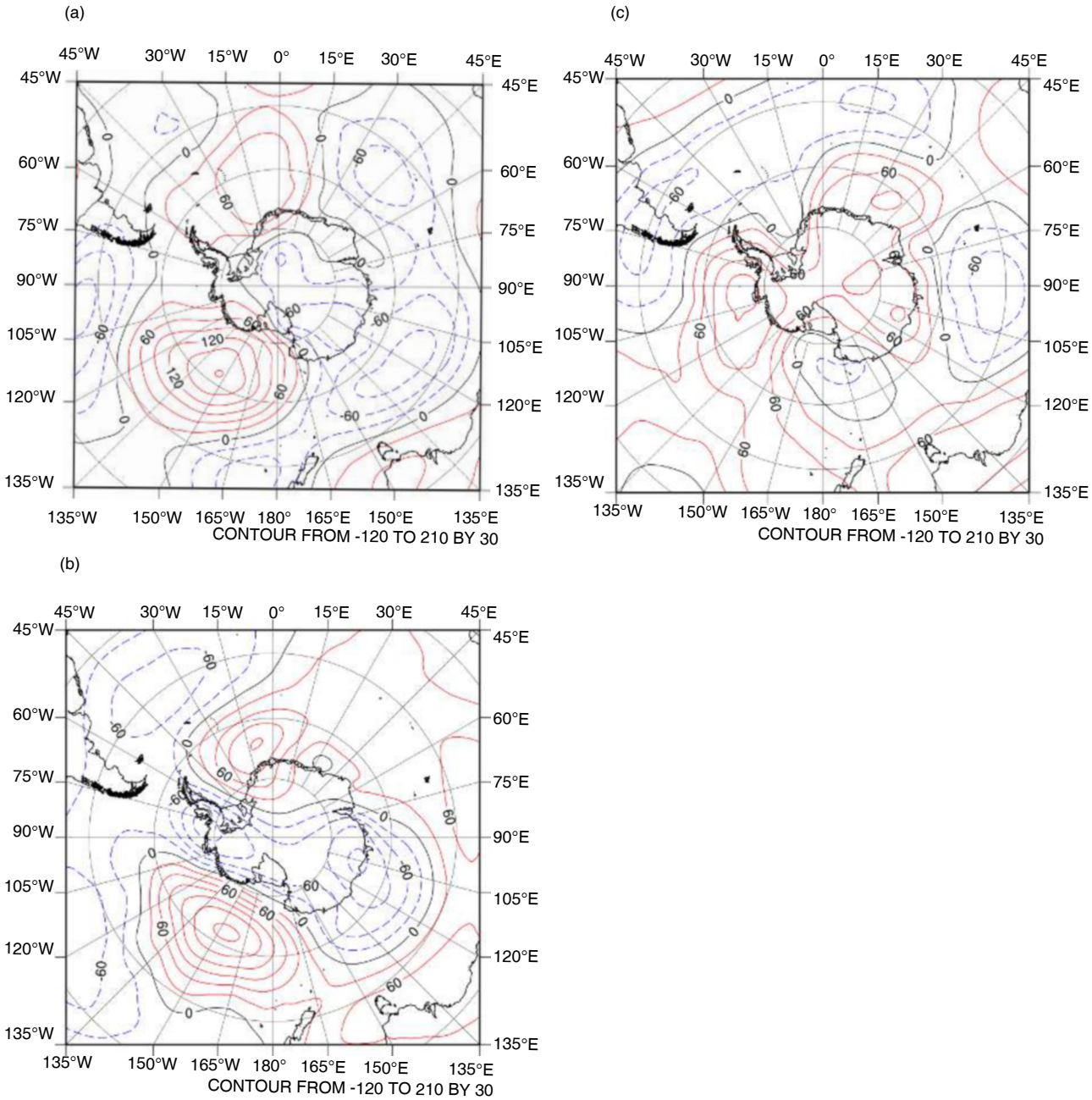

Fig. 3. ERA5 monthly 500-hPa geopotential height anomalies contoured every 30 m from −120 to 210 m for (a) July, (b) August, and (c) September.

anomaly in the Ross Sea persisted from July. In September, the anomalies virtually flipped signs, as there were positive anomalies across almost the entirety of the Antarctic continent (Fig. 3c).

The 500-hPa composite geopotential height anomalies during the four specified cold periods (Fig. 4) show large negative anomalies collocated with regions that observed extreme cold temperatures. For the first cold phase, 21–23 July, the composite geopotential height anomalies (Fig. 4a) indicate negative anomalies over most of East Antarctica, centered over Dome C and stretching over the East Antarctic Coast and RIS. A strong, positive height anomaly is located in the northern Ross Sea, with another region of positive height anomalies in the Bellingshausen Sea, west of the Antarctic Peninsula. The regions of negative height anomalies coincide with when temperatures at Zhongshan Station and Taishan AWS (Fig. 2) in East Antarctica decreased rapidly, and the cold persisted for the remainder of July. On RIS, temperatures at Margaret AWS (Fig. 2e) around this time decreased from approximately −50°C to −58.6°C at 1640 UTC 21 July. In the Weddell Sea, strong negative geopotential height anomalies suggest cold, southerly flow over the Peninsula and Great Wall Station (Fig. 2a), coinciding with a

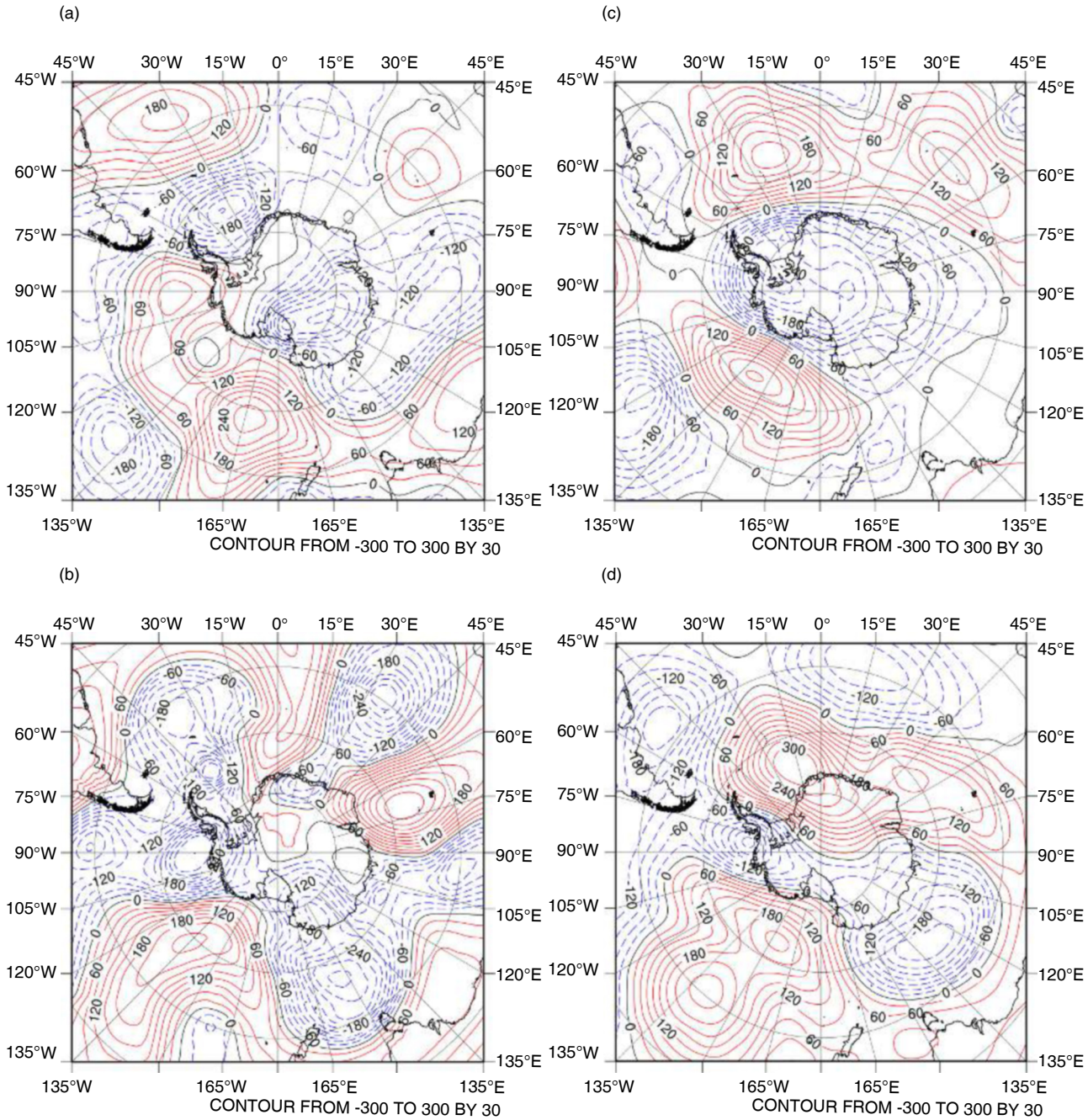

Fig. 4. ERA5 500-hPa anomalies during the four main cold phases contoured every 30 m from −300 to 300 m for (a) 21–23 July, (b) 31 July–1 August, (c) 10–13 August, and (d) 19–24 August.

period of cold temperatures during the first cold period. In WA, Byrd AWS (Fig. 2f) is located approximately between positive and negative geopotential height anomalies. This suggests calm weather conditions and was when Byrd AWS observed a local minimum temperature of −51.8°C at 1930 UTC 24 July.

During the second cold phase (31 July–1 August), the 500-hPa composite geopotential height anomalies (Fig. 4b) show negative height anomalies over most of the Antarctic continent. Positive height anomalies are centered north of the West Antarctic coast in the northwestern Amundsen Sea. A region of negative height anomalies was present from East Antarctica and Wilkes Land across RIS. As such, Zhongshan Station (Fig. 2c) observed its minimum temperature during this study period of −36.9°C at 1500 UTC 31 July. Just prior to this time period, on the western side of RIS near Ross Island and the USAP Airfields, Windless Bight AWS (Fig. 2d) observed a local minimum temperature of −53.4°C at 2210 UTC 29 July. Just after this time period, on the eastern side of RIS, Margaret AWS (Fig. 2e) observed a local minimum temperature of −60.4°C at 1310 UTC 1 August. In the Bellingshausen Sea, a region of negative geopotential height anomalies was centered and reached over the Antarctic Peninsula. Near the beginning of this time period, Great Wall Station (Fig. 2a) on the Peninsula observed a local minimum temperature of −9.8°C at 0300 UTC 30 July. In the middle of the East Antarctic Plateau near Taishan AWS, 500-hPa geopotential height anomalies were near 0 and Taishan AWS temperatures observed a local maximum of −41.6°C at 0000 UTC 31 July.

Composite 500-hPa geopotential height anomalies during the third cold phase (10–13 August) show negative anomalies over the entire Antarctic continent (Fig. 4c), with local minima at the southern portion of the Antarctic Peninsula and near Taishan AWS in East Antarctica (Fig. 2b). A strong, positive anomaly was located in a similar location as the previous cold phase, in the northeastern Ross Sea and western portion of the Amundsen Sea. Over East Antarctica, temperature observations at Taishan AWS and Zhongshan Station (Fig. 2) show a persistent period of cold, with Taishan AWS measuring its coldest temperature of −59.8°C at 2000 UTC 8 August. Likewise, temperature observations at Windless Bight AWS and Margaret AWS on RIS, as well as Byrd AWS in WA (Fig. 2), indicate cooling trends during this time period, culminating in a record cold temperature observation at Windless Bight AWS of −59.5°C at 1510 UTC 12 August. Byrd AWS (Fig. 2f) also observed its coldest temperature of 2023 of −63.9°C at 0710 UTC 13 August, within 1°C of its record cold temperature. Temperature observations at Great Wall Station on the Antarctic Peninsula were near their average for July–August 2023, perhaps due to the implied zonal flow across the Peninsula, given the location of the nearby geopotential height anomaly minimum and ensuing anomaly height gradient over the Peninsula.

During the fourth and final cold phase (19–24 August), composite geopotential height anomalies indicate negative height anomalies in the far eastern Bellingshausen Sea and over the southern Antarctic Peninsula, and a broad region of negative height anomalies over portions of East Antarctica (Fig. 4d). Positive height anomalies, however, are shown over much of Enderby Land in East Antarctica and stretched into the Weddell Sea. As with the previous cold phases, a local maximum in geopotential height anomalies was situated in the eastern Ross Sea. At each of the locations in the study except Zhongshan Station, this cold phase marked a period of either cooling in temperature observations, or persistent and record-breaking cold temperatures. At Great Wall Station on the Antarctic Peninsula (Fig. 2a), temperatures began cooling at the end of this cold phase and decreased by 10°C. At Taishan AWS on the East Antarctic Plateau (Fig. 2b), temperatures began cooling prior to this cold phase and continued throughout, decreasing by 10°C–15°C. While temperatures at Zhongshan Station showed a cooling trend before and after this cold phase (Fig. 2c), they remained approximately steady or warmed during this cold phase. Geopotential height anomalies were near 0 m over RIS. The weak geopotential height anomaly gradients over RIS, due to its location between strong anomalies, suggest calm atmospheric conditions over RIS. At Windless Bight AWS on western RIS near Ross Island and at Byrd AWS in WA (Fig. 2d), temperatures remained persistently cold during this cold phase at approximately −50°C and −57°C, respectively. At Margaret AWS on eastern RIS (Fig. 2e), temperatures decreased at the beginning of this cold phase and remained extremely cold throughout, culminating in two record-coldest temperature observations at Margaret AWS: −66.0°C at 2320 UTC 20 August, then −66.4°C at 0930 UTC 21 August.

5. Discussion, summary and future work

5.1. *Impacts*

Extreme cold temperatures from East Antarctica toward RIS were recorded by AWSs from the UW-Madison AMRDC AWS and PANDA network during July and August of 2023. Temperature data from six stations (Fig. 2) were compared to ERA5 500-hPa geopotential height anomalies during the four main cold phases (21–23 July, 31 July–1 August, 10–13 August, and 19–24 August). These comparisons found an association between local geopotential height maxima and extreme cold temperatures recorded on the continent.

In August, the extreme cold weather affected aviation operations for the US Antarctic Program to Phoenix Airfield. WINFLY was delayed nearly 15 days owing to the inability of aircraft to operate in the cold temperatures below the −50°C threshold (Lazzara et al., 2012). This delay impacted shipment of cargo and personnel to McMurdo Station for the start of the 2023–2024 field season. Historically, WINFLY is conducted between the deep core of the kernlose winter and before the

stormy transition season into early austral spring. Mid-to-late August of 2023 into early September was too cold for flight operations, and then was immediately followed by stormy weather that also prevented flights going to the Antarctic. Only two flights arrived successfully at Phoenix Airfield, McMurdo Station during the 2023 WINFLY.

5.2. *Future directions*

A further investigation into the origin of these anomalies may be worthy of future pursuit. Considering the monthly 500-hPa geopotential height anomalies investigated in this study, the development of negative height anomalies, across the entire Antarctic, in August 2023 corresponded with when these extreme cold phases occurred. To investigate why, it may be necessary to study influences from other regions further afield. Prior research has shown that teleconnections of atmospheric phenomena between Antarctica and the tropics and Southern Hemisphere midlatitudes can influence Antarctic weather and climate (e.g., Fogt and Bromwich, 2006). Further investigation of these teleconnections, as well as any influence of climate signals such as El Niño–Southern Oscillation or the Southern Annular Mode, on these cold phases may elucidate how the atmospheric patterns developed. Additionally, the composite 500-hPa geopotential height anomalies during the four cold phases exhibited how the atmospheric environment and regions of extreme cold shifted and evolved from mid-July to August 2023. It could be beneficial for future Antarctic operations and weather and climate research to understand how the large-scale austral winter atmospheric environment can be established and lead to numerous extreme cold temperature events.

Acknowledgements. The authors acknowledge support from the US National Science Foundation (Grant Nos. 1924730, 2301362, and 2205398). Thanks to Art CAYETTE for his assistance and efforts with the Antarctic meteorological analysis.

REFERENCES

Cherry-Garrard, A., 1922: *The Worst Journey in the World*. Constable & Co., 446 pp.

Ding, M. H., and Coauthors, 2022: The PANDA automatic weather station network between the coast and Dome A, East Antarctica. *Earth System Science Data*, **14** (11), 5019--5035. http://doi.org/10.5194/essd-14-5019-2022.

Fogt, Ryan L. and D. H. Bromwich, 2006: Decadal variability of the ENSO teleconnection to the high-latitude South Pacific governed by coupling with the Southern Annular Mode. *J. Climate*, **19**, 979–997, https://doi.org/10.1175/JCLI3671.1.

Genthon, C., D. Six, V. Favier, M. Lazzara, and L. Keller, 2011: Atmospheric temperature measurement biases on the Antarctic Plateau. *J. Atmos. Oceanic Technol.*, **28**, 1598–1605, https://doi.org/10.1175/JTECH-D-11-00095.1.

Hersbach, H., and Coauthors, 2020: The ERA5 global reanalysis. *Quart. J. Roy. Meteor. Soc.*, **146**, 1999–2049, https://doi.org/10.1002/qj.3803.

Keller, L. M., K. J. Maloney, M. A. Lazzara, D. E. Mikolajczyk, and S. D. Battista, 2022: An investigation of extreme cold events at the South Pole. *J. Climate*, **35**, 1761–1772, https://doi.org/10.1175/JCLI-D-21-0404.1.

Lazzara, M. A., G. A. Weidner, L. M. Keller, J. E. Thom, and J. J. Cassano, 2012: Antarctic automatic weather station program: 30 years of polar observation. *Bull. Amer. Meteor. Soc.*, **93**, 1519–1537, https://doi.org/10.1175/BAMS-D-11-00015.1.

Skansi, M., and Coauthors, 2017: Evaluating highest temperature extremes in the Antarctic. *Eos, Transactions American Geophysical Union*, **98**, https://doi.org/10.1029/2017EO068325.

Turner, J., H. Lu, J. King, G. J. Marshall, T. Phillips, D. Bannister, and S. Colwell, 2021: Extreme temperatures in the Antarctic. *J. Climate*, **34**, 2653–2668, https://doi.org/10.1175/JCLI-D-20-0538.1.

Turner, J., and Coauthors, 2004: The SCAR READER Project: Toward a high-quality database of mean Antarctic meteorological observations. *J. Climate*, **17**, 2890–2898, https://doi.org/10.1175/1520-0442(2004)017<2890:TSRPTA>2.0.CO;2.

Turner, J., and Coauthors, 2009: Record low surface air temperature at Vostok station, Antarctica. *J. Geophys. Res.: Atmos.*, **114**, D24102, https://doi.org/10.1029/2009JD012104.